



Warm measurements on cavities/HOMs

J. A. Mitchell ^{1,2}

¹Engineering Department, Lancaster University

²BE-RF Section, CERN

Graeme Burt

Rama Calaga

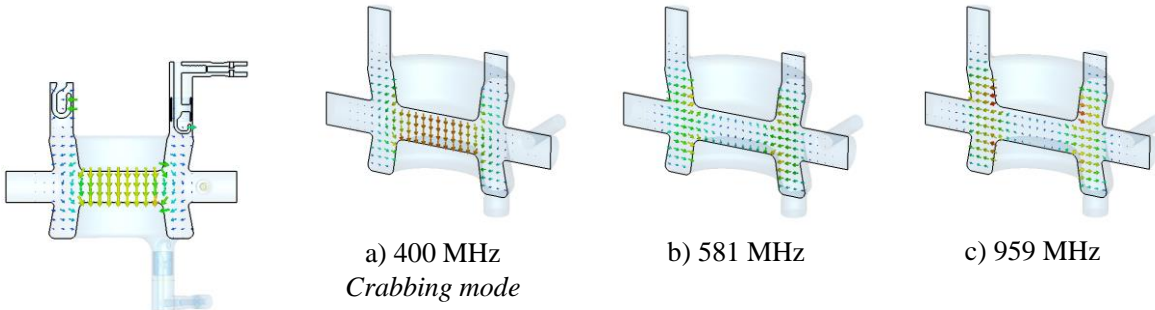
*6th HL-LHC Collaboration Meeting
Espace St Martin, Paris, 14-16 November 2016*



1. HOM coupler test boxes
 - HiLumi HOM couplers
 - RFD single coupler
 - L-bend transmission
 - Coaxial chamber
2. HOM coupler conditioning
3. Longitudinal measurements (DQW)
 - On-axis bead-pull
 - Multipole measurements
 - Stretched wire measurements
4. References

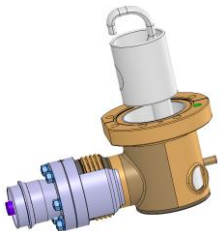
Higher Order Modes (HOMs)

- **Higher Order Modes (HOMs)**
- Modes of operation which occur at frequencies higher than the operational mode.
- If excited by an external source, the HOMs can deviate from the desired crabbing operation.



- HOM couplers damp the higher order modes to a load but whilst acting as a stop-band filter for the crabbing mode at **400 MHz**.

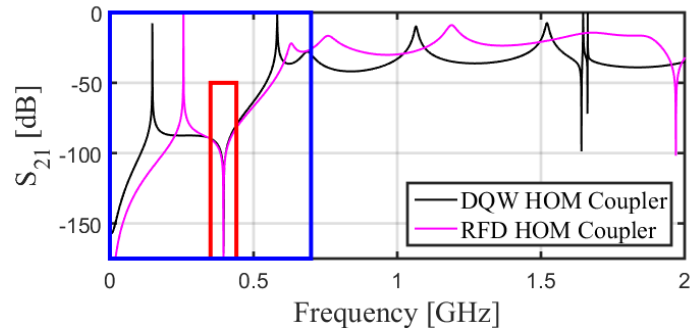
- The two HiLumi crab cavities to be tested in the SPS in 2018 are the Double Quarter Wave (DQW) and Radio Frequency Dipole (RFD).
- Each has HOM couplers with associated spectral responses tailored at providing a path at the HOM frequencies but acting as a stop-band to the crabbing mode.



a) SPS DQW HOM coupler

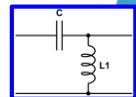
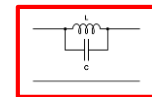


b) RFD HOM coupler

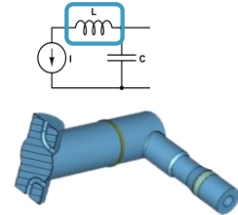
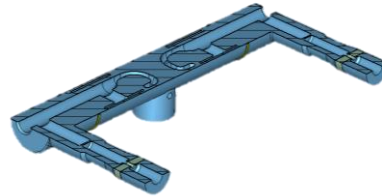
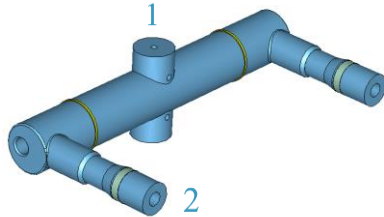


c) Spectral responses of the HOM couplers

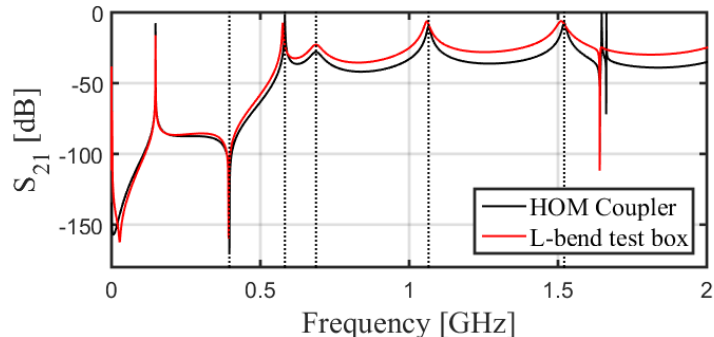
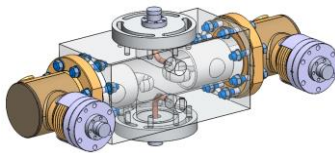
- It is beneficial to know the **spectral response** of the HOM couplers **pre-installation**.



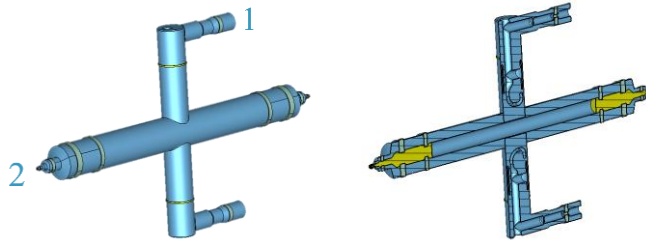
DQW L-bend transmission test box



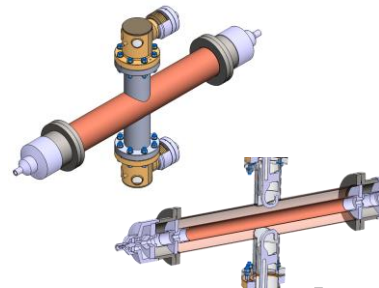
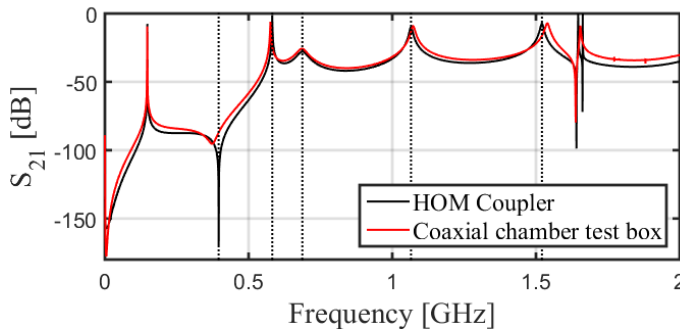
- Uses probes which preferentially use magnetic coupling to couple to the TE₁₁₀ waveguide mode in order to measure the spectral response.
- 2-port
 - Improves similarity of spectral response to that of the HOM coupler.
 - Allows the feasibility of high power conditioning to be investigated.



DQW coaxial chamber test box



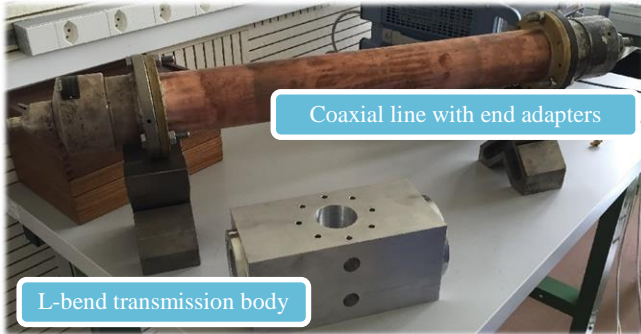
- Uses a **procured** coaxial line and connectors - reduction to 7-16/N-type.
- Peak frequencies not as accurate as L-bend, however simpler manufacture using procured components with documented operational tolerances.
- 2-port
 - Improves similarity of spectral response to that of the HOM coupler.
 - Allows the feasibility of high power conditioning to be investigated.



James Mitchell

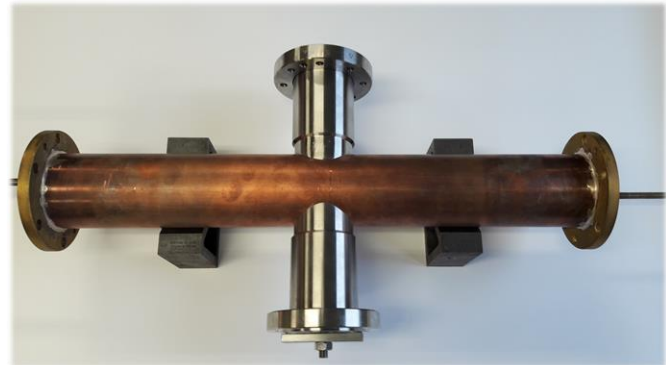
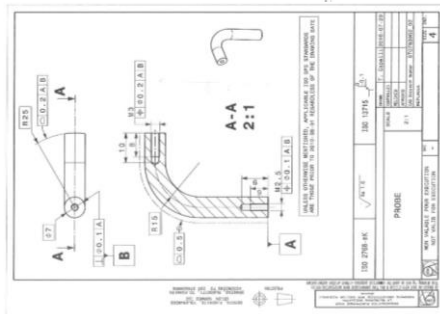
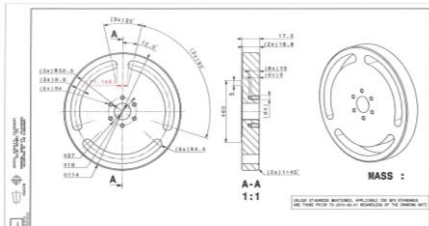
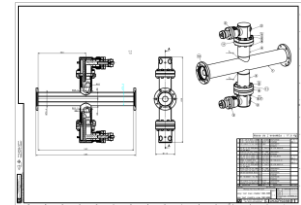
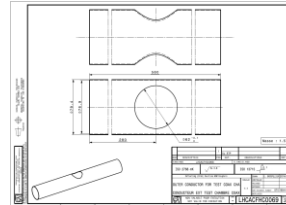
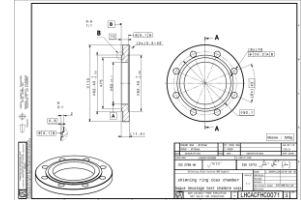
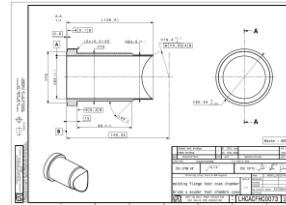
j.a.mitchell@lancaster.ac.uk – 15/11/16

DQW test box manufacture



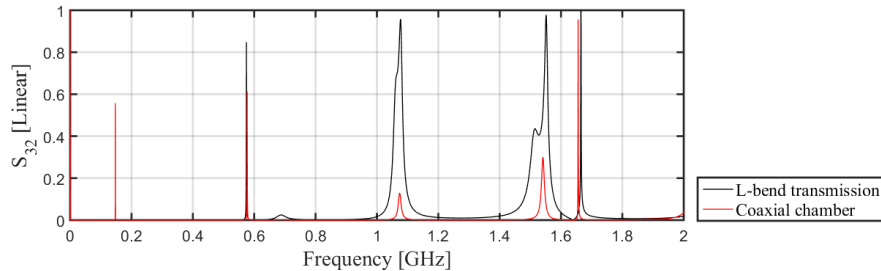
Coaxial line with end adapters

L-bend transmission body

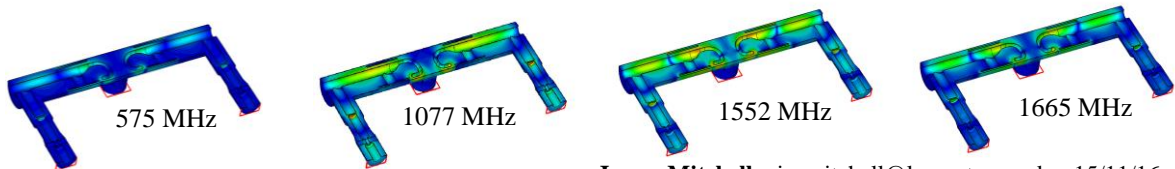


Coupler conditioning

- As the HOM couplers for the DQW are ‘on-cell’ there are areas of high field on the coupler surfaces.
- These areas can cause breakdown and heating of the HOM couplers.
- Hence, a device which can pre-condition the couplers prior to installation would be very valuable.

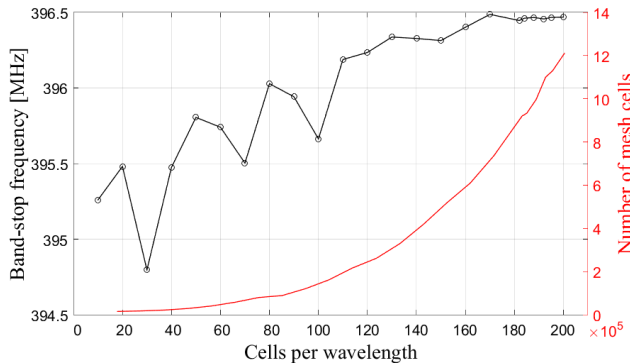
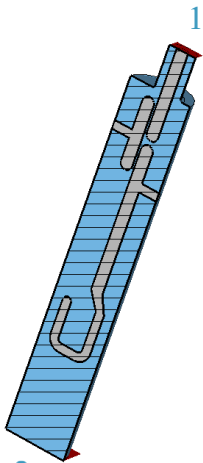


- In both cases, high transmission occurs at the frequencies of the HOM coupler interaction points.
- Areas of high field (i.e. deflecting mode and low Q_{ext} HOMs) should be investigated and the best conditioning configuration can be resulted.



RFD single coupler test box

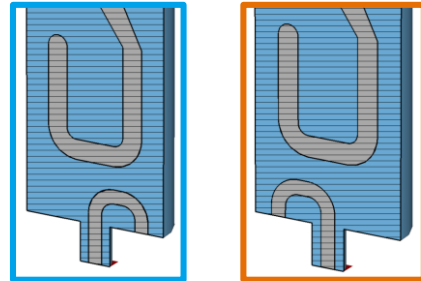
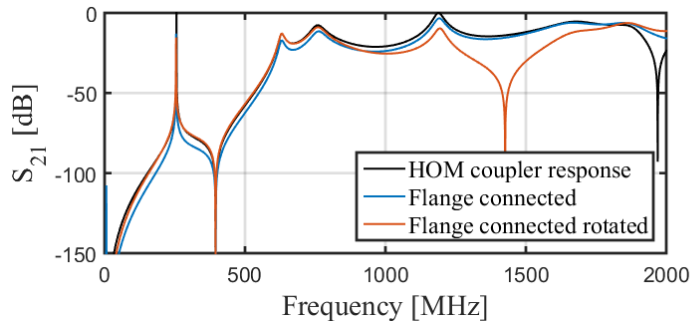
- For the RFD HOM coupler, a single probe test box has been designed.
- The structure's aim is to accurately **characterise the frequency of the stop-band filter**.
- To provide an accurate reference for the frequency of the stop-band, mesh convergence was necessary.



Peak	Frequency [MHz] (3dp)
1	255.840
2 (B-S)	396.487 ± 0.050
3	631.020
4	759.220
5	1189.000

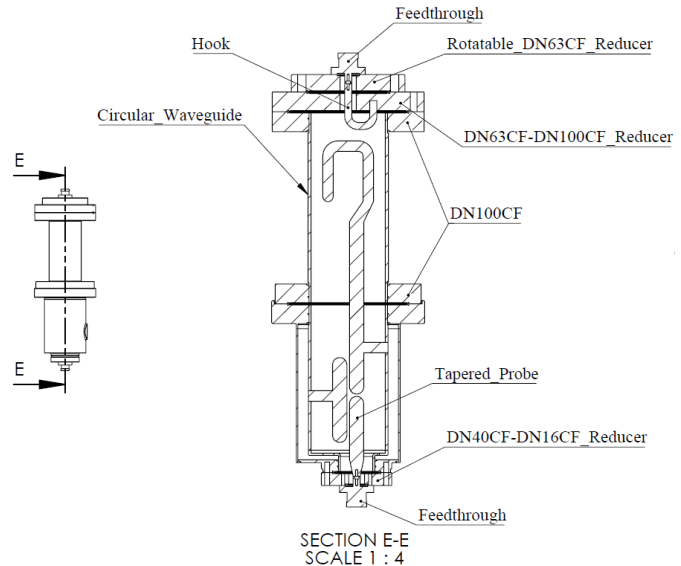
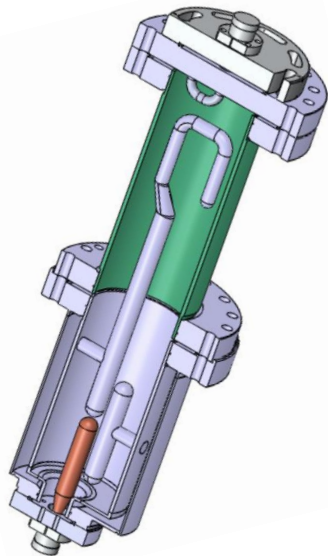
RFD single coupler test box

- Inductive connection to the wall of the waveguide is needed to diminish the TM_{010} waveguide mode and measure the response of the TE_{110} mode.
- The orientation of the pick-up also effects which waveguide mode is induced.



Peak	RFD HOM coupler frequency [MHz] (3dp)	Flange connected [MHz] (3dp)	Flange connected rotated [MHz] (3dp)
Stop-band	396.487 ± 0.050	396.567	396.443

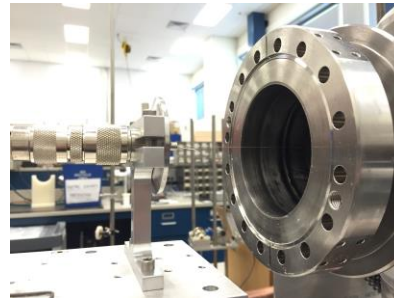
- Manufacturing drawings are currently being finalised.



- **Bead-pull**
 - On axis measurements to result in electric and magnetic field profiles.
 - Azimuthal measurements to try and quantify multipole components.
- **Stretched wire**
 - Allows the electrical centre to be established.
 - This data could then be referenced to the flange geometry for initial calibration.



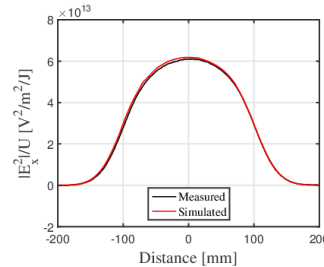
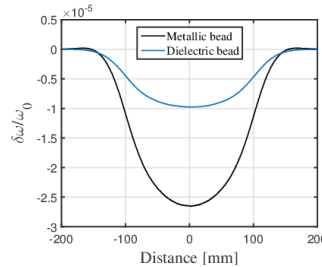
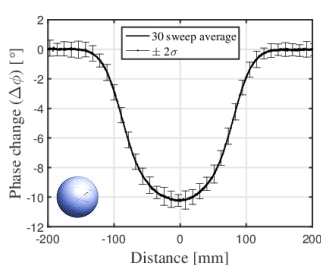
b) Multi-axis bead-pull set-up



b) Stretched wire set-up at JLAB

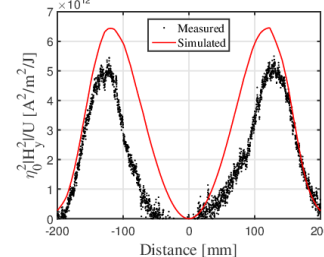
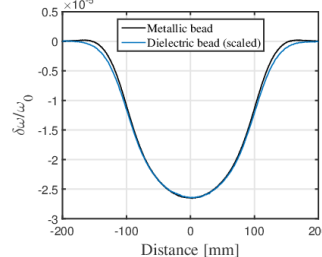
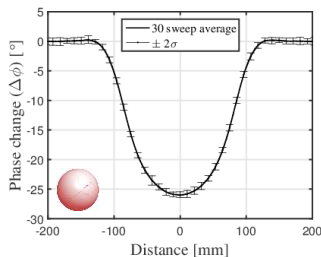
On-axis bead-pull

- 3-axis bead-pull set-up.
- Currently an **aluminium machined DQW PoP prototype** is being used to establish techniques **before analysing the Niobium cavities**.
- Metallic and dielectric beads allow electric and magnetic field profiles to be calculated.



Peak Value ratio
(measured/simulated)

98.8%



85.2%

Multipoles

- Multipole components can be calculated using a discrete number of longitudinal electric field profiles over an azimuth.
- Panofsky-Wenzel field decomposition can be used to calculate the multipole coefficients [2].

$$a_n = \frac{jn}{\omega\pi} \int_{-\pi}^{\pi} \frac{1}{r^n} \sin(n\theta) \int_{-l/2}^{l/2} e^{\left(\frac{j\omega z}{c}\right)} E_z(r, \theta, z) dz d\theta \quad (1)$$

$$b_n = \frac{jn}{\omega\pi} \int_{-\pi}^{\pi} \frac{1}{r^n} \cos(n\theta) \int_{-l/2}^{l/2} e^{\left(\frac{j\omega z}{c}\right)} E_z(r, \theta, z) dz d\theta \quad (2)$$

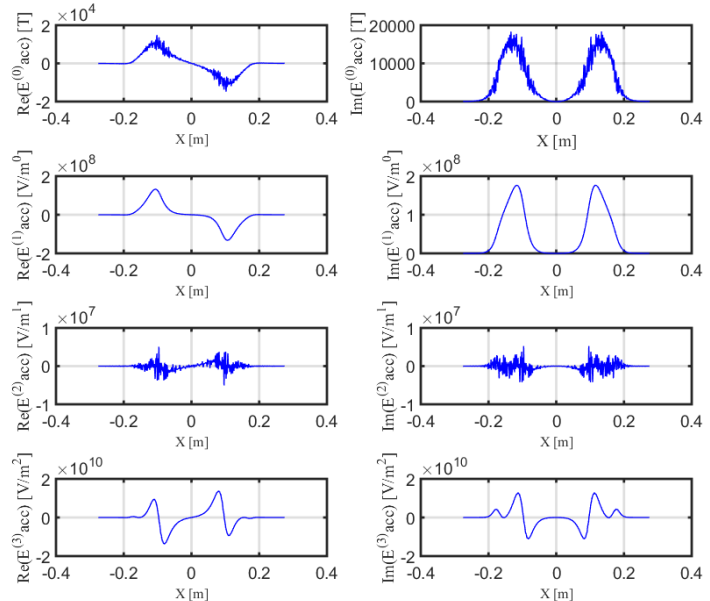
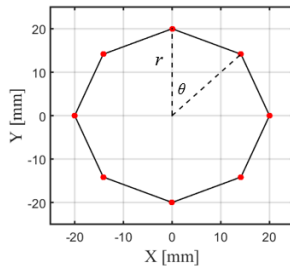
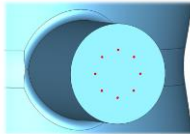
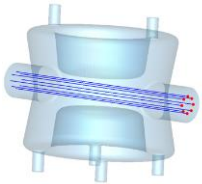
- Where n is the multipole number, i.e. $n = 0$ is the monopole, 1 is the dipole and 2 the quadrupole etc.
- r represents the radius at which the azimuthal integration takes place, z is the position along the longitudinal axis and E_z is the longitudinal electric field.

Multipole simulations

- In order to calculate the multipoles from simulation, a discrete number of longitudinal electric field profiles are taken over an azimuth at a specific radii.
- For visualisation of the multipole kicks, the field can be decomposed into E_{acc} for each of the multipole components.

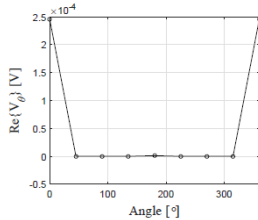
$$E_{acc} = e \left(\frac{j\omega z}{c} \right) E_z(r, \theta, z)$$

$$E_{acc}^{(n)} = j \int_{-\pi}^{\pi} \frac{1}{r^n} \cos(n\theta) E_{acc} d\theta$$

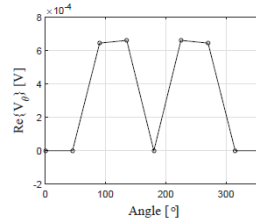


Normalised to 1J of stored energy in the cavity.

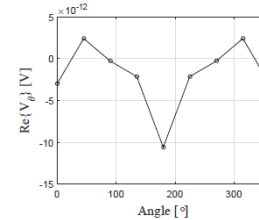
Multipole simulations



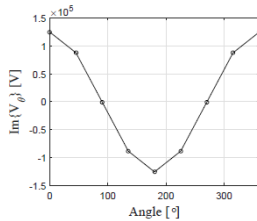
(a) $r = 15$ mm



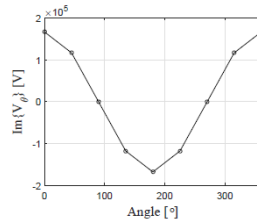
(b) $r = 20$ mm



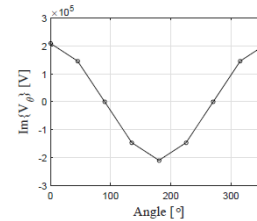
(c) $r = 25$ mm



(d) $r = 15$ mm



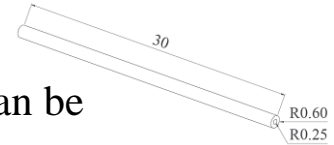
(e) $r = 20$ mm



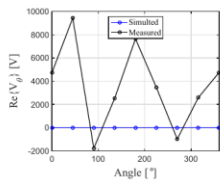
(f) $r = 25$ mm

	b_0	b_1	b_2	b_3
$\text{Re}\{b_n\}$	0.00E+00 ± 0.00	-3.33E+01 ± 1.74E-03	1.77E-01 ± 6.53E-02	-1.04E+03 ± 2.27E-01
$\text{Im}\{b_n\}$	0.00E+00 ± 0.00	1.01E-08 ± 3.26E-08	-1.41E-06 ± 4.47E-06	-1.89E-04 ± 1.76E-04

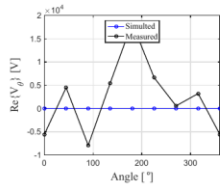
Multipole measurements



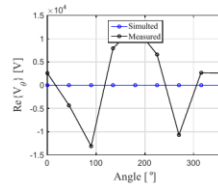
- By using a metallic needle the electric field on axis can be determined via bead-pull measurements.
- Following this, the same mathematics can be applied for multipole analysis.
- Initially this was trialled with a 30 mm needle at three radii with 8 points along the azimuth.



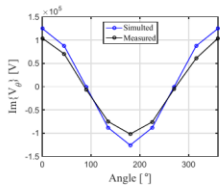
(a) $r = 15$ mm



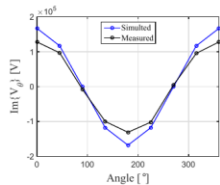
(b) $r = 20$ mm



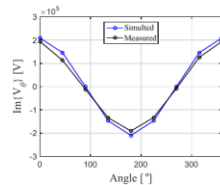
(c) $r = 25$ mm



(d) $r = 15$ mm



(e) $r = 20$ mm



(f) $r = 25$ mm

- Imaginary points gave a close representation of the simulated.
- However, difference due to the S/N ratio was too large for meaningful and repeatable multipole coefficients.

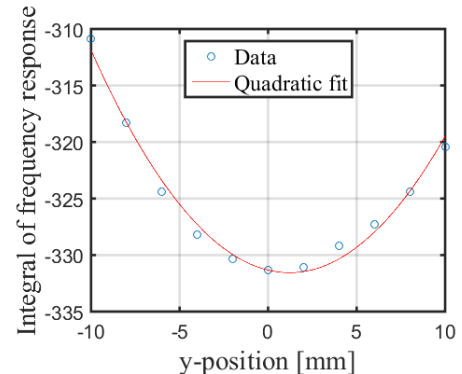
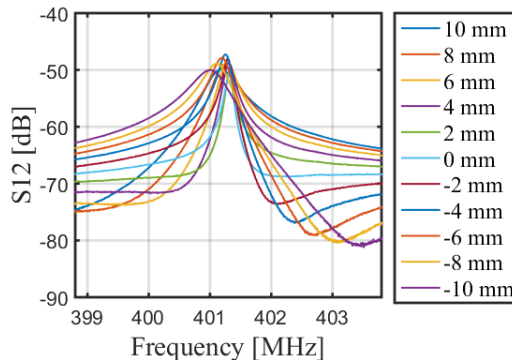
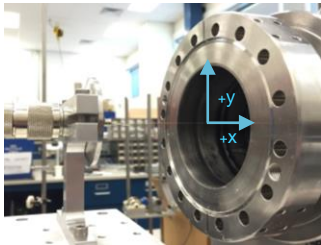
- Due to the similarity of the simulated and measured results, the feasibility of multipole measurements is shown.
- **Error analysis and propagation** should be applied to all data sets.
- After quantifying the error bars at the voltage stage **signal to noise reduction** techniques should be employed and **repeatability studies conducted**.

- ***Improve the S/N ratio!***
 - ✓ Orientate the pick-up loops at 90 degrees to the magnetic field.
 - Put higher power into the cavity amplifier/use cavity as attenuator.
 - ✓ Simulate over a larger number of points.




... Currently I am analysing a data set of 16 points at a radius of 30 mm with a larger field coupling from the pick-ups... results are looking promising.

Stretched wire measurements

- For DQW-NWV-002, stretched wire measurements were performed.
- The measurements allow the electrical centre of the cavity to be established [3].
- Using the **deflecting mode it is only possible** to see the centre in the **y-direction** – another mode should be used for the x-direction.



- For the measurements, there is an **observed asymmetry** due to an **impedance mismatch** – this mismatch would have to be eradicated for an accurate fit.
- This technique could be a powerful starting point for calibration to the electrical centre and lends itself well to the multi-axis set-up at CERN.
- To achieve this, **sensitive measurement equipment** should be installed, i.e. opto-couplers, which would allow reference to the geometric map.

-  J. A. Mitchell. *et al.*
LHC Crab Cavity Coupler Test Boxes
in Proc. IPAC16, Busan, Korea, May. 2016, paper WEPMB058, pp. 2248–2250.
-  Barranco García, J. *et al.*
Long term dynamics of the high luminosity Large Hadron Collider with crab cavities
in Phys. Rev. Accel. Beams, Oct. 2016, Vol 19, Issue 10, pp. 101003–101012.
-  Wang, H.
Wire stretching technique for measuring RF crabbing/deflecting cavity electrical center and a demonstration experiment on its accuracy
Not yet published.

Special thanks

E. Montesinos
A. Boucherie
T. Capelli
H. Wang